RESEARCH ARTICLE

A Haloing Structured SiMPs@Cu Composite Anode Material for Lithium Ion Batteries

Hui Xu[1,2,3], Xiaolan Wang[1,2,3], Rui Chen[1,2,3], Hui Zhang[1,2,3], Yong Wang[1,2,3], Hong Jin[2,3,*], Yu Bai[1,2,3,*], Ping Zong[2,3,*]

[1]State Key Laboratory for Mechanical Behaviour of Materials, Xi'an Jiaotong University, Xi'an, Shaanxi 710049, People's Republic of China
[2]Xi’an Jiaotong University Suzhou Academy, Suzhou 215123, People’s Republic of China
[3]School of Nano-Science and Nano-Engineering, Xi’an Jiaotong University, Suzhou 215123, People’s Republic of China

***Corresponding author: E-mail: jhjinhong@xjtu.edu.cn (Hong Jin)**

DOI: 10.5185/amp.2020.020399

Micrometer sized silicon particles encapsulated in copper layer (SiMPs@Cu) was synthesized by a simple electroless deposition process. The pH values, copper salt concentrations and the complexing agent concentration were studied to evaluate the factors which affected the copper layer structures. The micro sized Si particles were uniformly surrounded by a layer of Cu nanoparticles which can construct a conductive network within the electrode. The final composite SiMP@Cu can be obtained after H_2 treatment with a microstructure well maintained. The electrochemical properties of the composite were characterized in terms of Cyclic Voltammetry (CV), Gavanostatic charge/discharge (GCD) and Electrochemical Impedance spectroscopy (EIS). The SiMPs@Cu prepared at pH5 and with a concentration of 0.32 M Cu salt and 0.1 M complexing agent exhibited a improved specific capacity of more than 500 mA/g (at a current density of 100 mA/g) after 200 cycles, which is much better than the SiMPs without copper deposition. The result demonstrates that the copper layer can effectively alleviate the failure issue of electrode induced by Si pulverization during the charge/discharge process. This method is cost-effective and easy-to-control which illuminates a feasible strategy to fabricate Si anode with cheap micro sized Si starting material.

Introduction

There has been a great deal of research interest in the development of safe, good cyclability Li-ion batteries to satisfy the increasing needs of portable electronic products, energy-efficient devices, electric vehicle applications [**1-5**]. High specific energy can be achieved by utilizing electrode materials that have a high specific capacity. Silicon based anodes are considered to be one of the most promising candidates for the next generation high energy density lithium-ion batteries because of its high theoretical capacity (3590mAh/g for the $Li1_5Si_4$ phase at room temperature) and a relatively low lithium insertion potential (~0.4V vs. Li/Li^+) [**6, 7**]. However, the application of the silicon anode is still hindered by several major challenges: the low intrinsic electric conductivity, severe Si particle volume changes during lithiation/ delithiation processes, and unstable SEI (solid electrolyte interphase) on the surface of silicon particles caused by repeated volume changes. Large volume changes during cycling will produce significant stress inside the silicon particles which may lead to the Si particle (larger than the critical size) pulverization. It will result in the fracture of the electrode materials from the metal current collector and loss of electrical contact, subsequently the failure of silicon electrode structure with rapid capacity fading [**7-8**]. In order to maximize the potential of silicon anode, various approaches have been developed to solve the structural instability problems of Si-based electrode. These approaches are generally focusing on the following strategies or the integration of them: 1) Compositing silicon with conductive phases or networks to improve the conductivity of the anode [**9-12**]; 2) Applying a or several layer of coatings on the surface of silicon materials to restrict the continuous growth of SEI; 3) Inducing void space to accommodate Si particles volume expansion [**13, 14**]. Though the introducing of the nanostructures for instance silicon nanoparticles, nanowires or thin films can noticeably avoid pulverization and subsequently improve the cycling performance of the silicon-based anode material, it is still worth developing optimized silicon anode by micro sized Si particles (SiMPs) due to its higher energy density, less agglomeration trend as well as the much lower cost of in terms of the real application.

For electrode constructed by micro sized Si particles, the pulverization process of SiMPs may induce continuous growth of solid electrolyte interphase layer which will consequently reduce the coulombic efficiency for the first few cycles and lead to sharp capacity decay [**8**]. Therefore, to achieve stabilized structure is one of the key aspects for solving the rapid capacity fading. Many studies have developed Si–based composites to stabilize the silicon structure and enhance electric conductivity of silicon materials, thus to improve the lithium storage properties [**15**]. Such as pomegranate-inspired design [**13**], double-walled Si/SiO_2 hollow tubes [**16**], Si-Fe based nanocomposite [**17**] and silicon/copper composite [**4,11,18**]. Among them, compositing Si particles with metal materials is a feasible strategy which can not only significantly enhance the electrical conductivity of anode but also can easily tune the hybrid structure by controlling fabrication process. N. Fukata *et. al.*, [**17**] have synthesized Si-Fe based materials connected by Ge nanostructures using chemical vapor deposition. The advantage of the structure is obvious because the internal voids created by the aggregation of nanoparticles can accommodate the volume expansion and release the mechanical stress during the electrochemical lithiation process. This has led to an stable cyclic properties that survives 110 cycles at 0.1 C charge/discharge rate while maintaining a discharge capacity about 630.0 mAh/g. Some investigations have been done to prepare Si-Cu composites for the anode [**18-22**], however most of them involved complicated preparing methods or based on the nanosized raw materials. To develop simple and low-cost fabricating techniques for Si anode is worthwhile studying. Cetinkaya *et. al.*, [**4**] have employed the electroless deposition technique to prepare a silicon/copper composite. The mesoporous nature of the copper layer facilitate the diffusion of Li ions along with the enhanced conductivity of silicon particles. Results shown that the specific capacity of copper coated silicon is better than that of virginal Si, but the gradual decay during the cycling still happen, which indicates that the copper shell formed in this study remains to be further improvement.

Attempts to use Si microparticles as cheap starting materials, here we design a simple, low cost and easy to implement electroless method to synthesis core/shell structural SiMPs@Cu composite for Li-ion battery anode. Copper nanoparticles are uniformly deposited round the micro silicon particles, offering advantages. Despite pulverization of SiMPs during cycling, the coated copper nanoparticles can still ensure electrical contact with SiMPs and maintain a conductive network within the electrode. The SiMPs@Cu composite core/shell structure is expected to solve the problem of structure fracture and low electrical conductivity, demonstrating improved battery performance for SiMPs as the anode of lithium ion battery.

Experimental

In this study, the silicon powders (purity 99.9%, ~1µm diameters in average size) used to produce SiMPs@Cu composite powders are supplied from Aladdin. Before producing the SiMPs@Cu composite powders using an electroless coating method, the surfaces of the SiMPs are pretreated. First, the surfaces of the silicon powders form a very thin layer of polydopamine that helps the Cu-nucleation seed adhere more readily to the SiMPs surface. Then, the surfaces of the silicon powders were sensitized with 5g/l $SnCl_2$, 10ml/l HCl solution under magnetic stirring for 1h. The silicon powders were then activated in a solution containing 0.5g/l $PdCl_2$, 6.25ml/l HCl with a magnetic stirrer for 1h. Finally, the silicon powders were filtered and washed with distilled water several times. After the pretreatment process, the surfaces of the silicon powders were coated with copper using an electroless process. An electroless bath was prepared using a $CuSO_4·5H_2O$ precursor, and then Dimethylamine-Borane (DMAB) is added to the solution. The pH value of the solution was controlled using $NH_3·H_2O$. The solution was stirred with a magnetic stirrer for 1h, then standing for 12h to make SiMPs@Cu settle down and centrifuge to get SiMPs@Cu composite powders, the powders are washed with distilled water and ethanol and dried at 60°C in a vacuum oven for 12 h. The whole experiment was carried out at room temperature [**15**]. Final, H_2 atmosphere annealing at 600°C was applied to form SiMPs@Cu core–shell structure.

The final materials were characterized by scanning electron microscopy (SEM, JEOL JM3-6390) and Transmission Electron Microscopy (TEM, FEI Tecnai G2 F20 S-TWIN). The structure of the as-prepared nanoparticles were analyzed by X-ray Diffraction (XRD, Bruker D8 ADVANCE) Cu Ka radiation (1.5406 Å) to identify the phase and elemental composition of materials.

Electrochemical performances of SiMPs@Cu composite powders were investigated with two-electrode coin-type cells (CR 2032). The working electrode was prepared through a complex processing for a slurry coating. The slurry consists of 80 wt.% SiMPs@Cu composite powders, 10 wt.% super P conductive black and 10 wt.% polyvinylidenefluotide (PVDF) dissolved in N-methyl pyrrolidinone (NMP), was coated in the copper coils. Test cell was assembled in an argon-filled glove box. The counter electrode and the reference electrode were the lithium foil. The electrolyte consisted of 1M $LiPF_6$ dissolved in 1:1 (in volume) of ethylene carbonate (EC) and dimethyl carbonate (DMC). The separator was the polypropylene (PP) micro-porous film (Cellgard 2400).

The galvanostatic charge-discharge test was carried on Neware CT-3008-S4 at a rate of 1C (1C=100mA/g) in the voltage range of 0.01 V to 1V (versus Li/Li^+). The Cycling Voltammetry (CV) was tested by CHI600E electrochemical working station at a scan rate of 50 mV/s in the voltage of 0.01 V to 1 V at a room temperature (T=25°C).

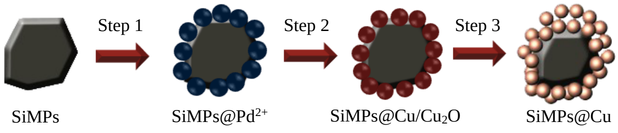

Fig. 1. Schematic illustration of the synthesis process of SiMPs@Cu composite.

The fabrication process of SiMPs@Cu composite core/shell anode structure has been schematically illustrated in **Fig. 1**. First, after pretreatment, Pd^{2+} was adsorbed on the surface of the SiMPs. Then, it was followed by copper plating process and obtained Cu and Cu_2O coated SiMPs (SiMPs@Cu/Cu_2O). Finally, to transform the SiMPs@Cu/Cu_2O core–shell structure into SiMPs@Cu, H_2 atmosphere annealing at 600 °C was applied that reduced the Cu_2O into Cu, thus forming SiMPs@Cu core–shell structure.

Results and discussion

The morphology of the irregularly sized pristine SiMPs (1μm diameters in size) is shown in **Fig. 2(a)**. After copper electroplating process, a layer of fine Cu/Cu_2O particles can be seen coated on the SiMPs in **Fig. 2(b-e)**. By adjusting the fabricating parameters including pH, copper salt concentration and complexing agent content, the morphology of the composite various in some degree. The SEM images reveal that colloid pH and Cu salt concentration play important roles on the morphology of the Cu coatings. Composites prepared at pH5 with higher Cu salt concentration (0.32 M) and 0.05 M complexing agent display a relatively continuous uniform and dense Cu/Cu_2O layer on the surface of SiMPs (**Fig. 2(e)**). After treated by H_2 reduction, **Fig. 2(f)** suggested that the SiMPs@Cu composite maintained similar microstructure during reduction treatment.

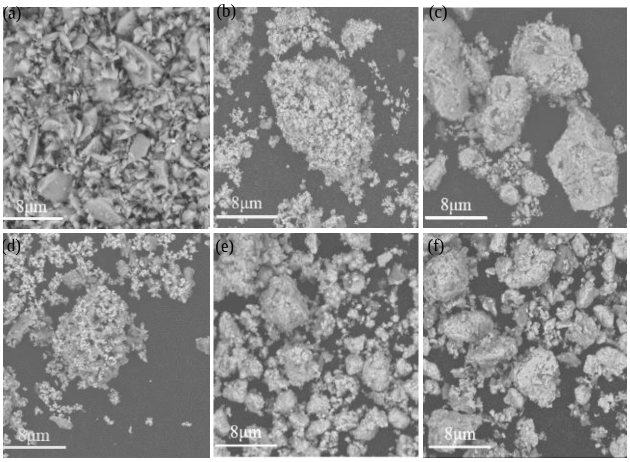

Fig. 2. SEM images of SiMPs, SiMPs@Cu/Cu_2O, SiMPs@Cu composite at different conditions; (a) the SEM of SiMPs; (b) SEM images of pH5, 0.20 M Cu^{2+}, 0.05 M complexing agent; (c) SEM images of pH5, 0.32 M Cu^{2+}, 0.1 M complexing agent; (d) SEM images of pH11, 0.32 M Cu^{2+}, 0.05 M complexing agent; (e) SEM images of pH5, 0.32 M Cu^{2+}, 0.05 M complexing agent; (f) SEM images of reducing Cu_2O.

The microstructure of **Fig. 2(c)** and **Fig. 2(f)** was further investigated by TEM (**Fig. 3**). **Fig. 3(a)** shows a TEM image of an individual Si micro particle which was uniformly surrounded by nano sized Cu particles. The magnified TEM image shows that the thickness of the copper layer is around 100 nm, which demonstrates that copper coated micro silicon structure is obtained successfully. After reducing Cu_2O with H_2, nano-sized Cu particles connect to each other and form a denser layer around SiMPs. The Cu layer coated on the Si surface can construct a conductive network to improve the electrical connections between SiMPs during cycling process.

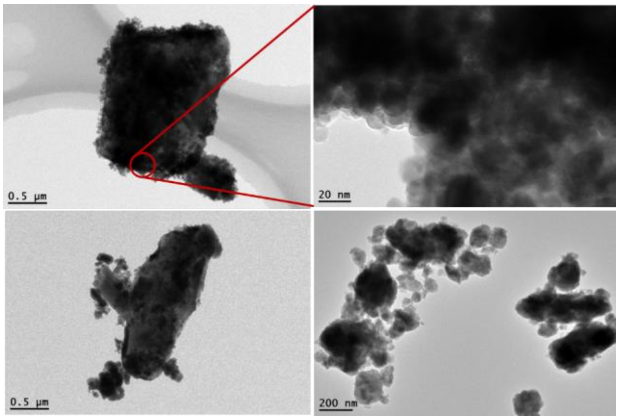

Fig. 3. TEM images of SiMPs@Cu/Cu_2O, SiMPs@Cu composite; (a) TEM images of pH5, 0.32 M Cu^{2+}, 0.1 M complexing agent; (b) TEM images of reducing Cu_2O.

The phase composition of the copper coated SiMPs samples is characterized by X-ray diffraction (XRD). As **Fig. 4** shown, The typical reflection peaks at 2θ values of 28°, 47°, 59°, 69°, and 76° can be indexed to the f.c.c. silicon structure (JCPDS No.27-1402) [**4**]. The Bragg reflection at 2θ=36°corresponding to the (111) plane of Cu_2O shows a broad width, which suggests that the grain size of Cu_2O tends to nanoscale [**23**]. The crystallization peaks observed at 43.6°, 50.5°, and 74.5° of the copper coated SiMPs samples correspond to the (111), (200), and (220) planes of fcc crystal structures of metallic Cu[4]. After reducing SiMPs@Cu/Cu_2O with hydrogen, the diffraction peak of copper becomes sharper and no Cu_2O peak was detected, implying the completed reduction of Cu_2O to Cu with further crystallization of the copper grains which is corresponding to the TEM results.

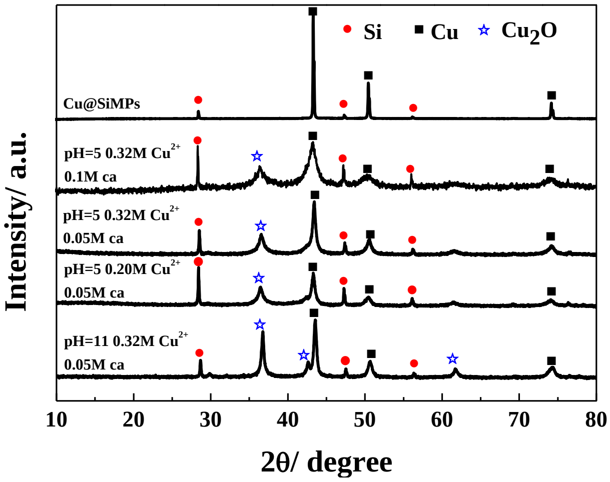

Fig. 4. XRD patterns of SiMPs@Cu/Cu_2O,SiMPs@Cu composite at different conditions.

It is known that the electrochemical performance of the electrode materials is highly influenced by the interfacial charge transfer process and the lithium ion diffusion in active materials. To further investigate the kinetics process during charge/discharge cycles, EIS was employed to characterize the impedance properties of the copper coated micro silicon with and without Cu_2O and the results are presented in **Fig. 5**, all the plots are composed of depressed semicircles in the high frequency range and an inclined linear curve in the low frequency zone. The diameter of the semicircle is usually assigned to the combination of a solid/electrolyte interface resistance and charge transfer impedance in the active layer, while the inclined line represents kinetic properties of Li-ion diffusion in the anode materials [**4**]. Compared to pristine SiMPs, the other samples present smaller diameters at the high frequency region which demonstrates that the electroless deposition can effectively enhance the conductivity of the micrometer size silicon anode. And most the slopes of the linear curve are higher than the original SiMPs anode, which illustrates that the presence of copper in the composites facilitate the Li-ion diffusion in the electrode.

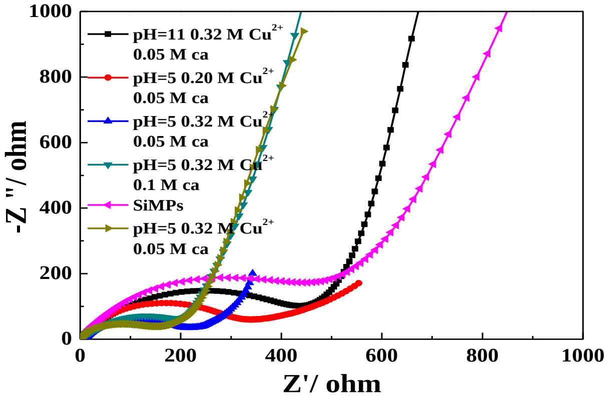

Fig. 5. Nyquist plots of the cells with SiMPs, SiMPs @ Cu/Cu_2O, SiMPs@Cu composite electrodes at different conditions.

The cycling stability at 0.1 A/g of electrodes made of pristine SiMPs, SiMPs@Cu/Cu_2O and SiMPs@Cu composites are evaluated by galvanostatic discharge–charge measurement in the voltage range of 0.01-1V, as exhibited in **Fig. 6(a)**. It is noted that the capacity of the pristine SiMPs electrode decreases rapidly after only a few cycles. It is reported that micro sized Si particles suffer from pulverization due to the large volume change during cycling, inducing excessive growth of the solid-electrolyte interface (SEI) layer and electrode material peeling off from the metal current collector. Compared with the pristine SiMPs electrode, both the SiMPs@Cu/Cu_2O and SiMPs@Cu electrode show better cycling performance. According to the Si content in the composite, The capacity retention of the SiMPs@ Cu/Cu_2O electrode after 50 cycles at 0.1 M complexing agent, 0.32 M copper ion concentration and pH=5 delivers a specific capacity of 387.3 mAh/g. As the Cu_2O reduced by H_2, the SiMPs@Cu core–shell structure can be formed. And the SiMPs@Cu shows a better electrochemical property. The first discharge and charge deliver a specific capacity of 3518.1 and 1753.2 mA h/g, respectively. The initial irreversible capacity is caused by the formation of SEI membrane. As shown in **Fig. 6(b)**, the SiMPs@Cu electrode maintains a high specific capacity over 500 mAh/g even after 200 cycles. This is much better than the pristine silicon anode based on the microsized Si particles, and also displays noticeable performance compared with other Si-Cu anodes from literatures (**Table 1**). The rate capability was investigated at the current density ranging from 0.1 to 0.5A/g, as shown in **Fig. 6(c)**. The SiMPs@Cu composite electrode exhibits the average capacity of 1446.5, 495.2 and 294.3mAh/g at the current density of 0.1, 0.3 and 0.5A/g, respectively. The SiMPs@Cu composite electrode presents a good capacity recovery stability. As the current density switches back from 0.5 A/g to 0.1 A/g, the high reversible capacity of 507.2 mAh/g can be recovered. We also noticed that the corresponding coulombic efficiency quickly increases to 95% at the fourth cycle and then reaches up to 97.5% after eight cycles.

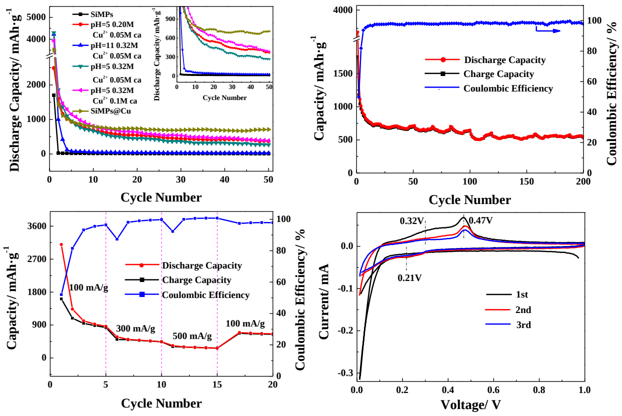

Fig. 6. (a) Electrochemical performance of SiMPs, SiMPs @ Cu/Cu_2O, SiMPs@Cu composite electrodes at different conditions; (b) Charge/ discharge capacity of SiMPs@Cu electrode at 1C (1C = 100mA/g) as well as the coulombic efficiency; (c) Charge/discharge capacity of SiMPs@Cu electrode at various rates from 1C to 5C; (d) Cyclic voltammetry curves of SiMPs@Cu composite electrode in the potential window between 0.01 V to 1 V at the rate of 50 mV/s.

Table 1. Comparison of Si-Cu anodes performance.

Materials and Structure	Technique	Current density	Cycles	Capacity	Ref.
Cu particles coated on SiMPs	Electroless deposition	100 mA/g	200	500 mAh/g	This work
Cu (diameter 100nm) coated on the etched Si particles with Cu_3Si on interface	Electroless deposition	100 mA/g	15	1000 mAh/g	19
Cu layer (100nm in thickness) covers on the Si powders	Electroless process	100 mA/g	20	240 mAh/g	4
Hollow Si–Cu alloy nanotubes	PECVD. with H2 annealing	3.4 A /g	1000	1010 mAh/g	18
Cu-Si nanowires	molten salt electrolysis	200 mA/g	200	601.3 mAh/g	20
Si@Cu3Si (Cu) nanowires/ nanorods/ nanocapsules	High-energy arc plasma through VLS growth	100 mA/g	100	783 mAh/g	21

The significant improvement in cycling performance of the SiMPs@Cu electrode suggests that Cu can accommodate the large volume expansion of SiMPs during cycling and the Cu framework is able to enhance the conductivity among SiMPs. Furthermore, the coating of Cu can prevent the contact between electrolyte and SiMPs. Electrochemical Li-ion storage performance of SiMPs@Cu were evaluated by CV measurement and shown in **Fig. 6(d)**. The measurements were performed from 0.01V to 1V versus Li/Li+ at a scan rate of 50 mV/s. In the discharge process, an obvious lithiation at peak 0.2-0.01V can be observed, which indicates the lithiation of silicon phase change from a crystalline to an amorphous structure. In the charge process, the peak at 0.25-0.5 V, respectively, which can be ascribed to the delithiation transition from LixSi to amorphous Si. It is reasonable to speculate that the electrochemical active substance in the anode is mainly attributed by SiMPs. Moreover, the CV curves of the second and third cycles are nearly repeatable. It implies the good reversibility and stability of the Li-ion intercalation and deintercalation during the charge/discharge process.

Overall, the good electrochemical performance of the as prepared SiMPs@Cu composite may be attributed to the following advantageous aspects. First, the SiMPs particles enables the composite to possess higher reversible capacity. Second, the Cu framework could not only buffer the volume change of the SiMPs particles, but also benefit the electronic and ionic conductivity, shorten the Li-ion diffusion path and facilitate the high rate capability.

Conclusion

In summary, SiMPs@Cu composite is successfully fabricated by a simple electroless coating method based on the microsized Si particles. The copper nanoparticles form a layer coated on the surface of the micro sized Si particles to construct a conductive network which effectively ensure the structure stability of anode during the charge/discharge process. As a result, the SiMPs@Cu anode prepared at pH5 with a concentration of 0.32 M Cu salt and 0.1 M complexing agent shows a optimal reversible capacity of more than 500 mAh/g after 200 cycles(at the current density of 100 mA/g), good rate capability and long-term cycling stability. This low cost and easy-to-use synthesize method can be adapted to prepare Si anode based on microsized raw materials which exhibits noticeable advantages in future real applications. Moreover, the coated Cu layer can be considered as the 3D current collector which provides a path to develop Cu foil free light electrodes. Lastly, this work provides an optional approach to solve the pulverization problem of Si anode and is also helpful for other materials with similar problems.

Acknowledgements

This work is sponsored by the Collaborative Innovation Center of Suzhou Nano Science and Technology, National Natural Science Foundation of Youth Science Fund China (No.21805221), Jiangsu Province Fundamental Research Grant (BK20150379, BK20160389). Suzhou City Key Industry Technological Innovation (Perspective Application Research) Grant (SYG201621).

Keywords

Lithium ion batteries, anode, SiMPs@Cu, electroless deposition.

Reference

1. Cao, X.; Chuan, X.; Massé, R. C.; Huang, D.; Li, S.; Cao, G.; *Journal of Materials Chemistry A*, **2015**, *3*, 22739.
2. Cetinkaya, T.; Uysal, M.; Akbulut, H.; *Applied Surface Science*, **2015**, *334*, 94.
3. Cetinkaya, T.; Uysal, M.; Guler, M. O.; Akbulut, H.; *International Journal of Hydrogen Energy*, **2014**, *39*, 21405.
4. Cetinkaya, T.; Uysal, M.; Guler, M. O.; Akbulut, H.; Alp, A.; *Powder Technology*, **2014**, *253*, 63.
5. Chan, C. K.; Peng, H.; Liu, G.; McIlwrath, K.; Zhang, X. F.; Huggins, R. A.; Cui, Y.; *Nature Nanotechnology*, **2008**, *3*, 31.
6. Ashuri, M.; He, Q.; Shaw, L. L.; *Nanoscale*, **2016**, *8*, 74.
7. Wu, H.; Cui, Y.; *Nano Today*, **2012**, *7*, 414.
8. Sun, Y.; Liu, N.; Cui, Y.; *Nature Energy*, **2016**, *1*.
9. Hwang, C.; Kim, T. H.; Cho, Y. G.; Kim, J.; Song, H. K.; *Scientific Reports*, **2015**, *5*, 8623.
10. Jaumann, T.; Herklotz, M.; Klose, M.; Pinkert, K.; Oswald, S.; Eckert, J.; Giebeler, L.; *Chemistry of Materials*, **2014**, *27*, 37.
11. Murugesan, S.; Harris, J. T.; Korgel, B. A.; Stevenson, K. J.; *Chemistry of Materials*, **2012**, *24*, 1306.
12. Zhong, L.; Beaudette, C.; Guo, J.; Bozhilov, K.; Mangolini, L.; *Scientific Reports*, **2016**, *6*, 30952.
13. Liu, N.; Lu, Z.; Zhao, J.; McDowell, M. T.; Lee, H. W.; Zhao, W.; Cui, Y.; *Nature Nanotechnology*, **2014**, *9*, 187.
14. Liu, N.; Wu, H.; McDowell, M. T.; Yao, Y.; Wang, C.; Cui, Y.; *Nano Letters*, **2012**, 12, 3315.
15. Li, Y.; Yan, K.; Lee, H.W.; Lu, Z.; Liu, N.; Cui, Y.; *Nature Energy*, **2016**, *1*, 15029.
16. Wu, H.; Chan, G.; Choi, J. W.; Ryu, I.; Yao, Y.; McDowell, M. T.; Lee, S. W.; Jackson, A.; Yang, Y.; Hu, L.; Cui, Y.; *Nature Nanotechnology*, **2012**, *7*, 310.
17. Fukata, N.; Mitome, M.; Bando, Y.; Wu, W.; Wang, Z. L.; *Nano Energy*, **2016**, *26*, 37.
18. Song, H.; Wang, H. X.; Lin, Z.; Jiang, X.; Yu, L.; Xu, J.; Yu, Z.; Zhang, X.; Liu, Y.; He, P.; Pan, L.; Shi, Y.; Zhou, H.; Chen, K.; *Advanced Functional Materials*, **2016**, *26*, 524.
19. Kim, J. W.; Ryu J. H.; Lee, Kyu T.; Seung M. Oh; *Journal of Power Sources*, **2005**, *147*, 227.
20. Zhou, Z. R.; Zhang, Y. J.; Hua, Y. X.; Dong, P.; Lin, Y.*; Xu, M. L.; Wang, D.; Li, X.; Han, L.; Duan, J. G.; *Journal of Alloys and Compounds*, **2018**, *751*, 307.
21. Liang, J. S.; Yang, Y. L.; Gao, J.; Zhou, L.; Gao, M.; et. al.; *Journal of Solid State Electrochemistry*, **2019**.
22. Zhang, H.; Zong, P.; Chen, M.; Jin, H.; Bai, Y.; Li, S. W.; Ma, F.; Xu, H.; Lian, K.; *ACS Nano*, **2019**, *13*, 3054.
23. Zhang, J.; Zhang, C.; Wu, S.; Liu, Z.; Zheng, J.; Zuo, Y.; Xue, C.; Li, C.; Cheng, B.; *Nanoscale Research Letters*, **2016**, *11*, 214.